地殼形變的各種觀測方法

GPS ： Global Positioning System

InSAR ： Interferometric Synthetic Aperture Radar

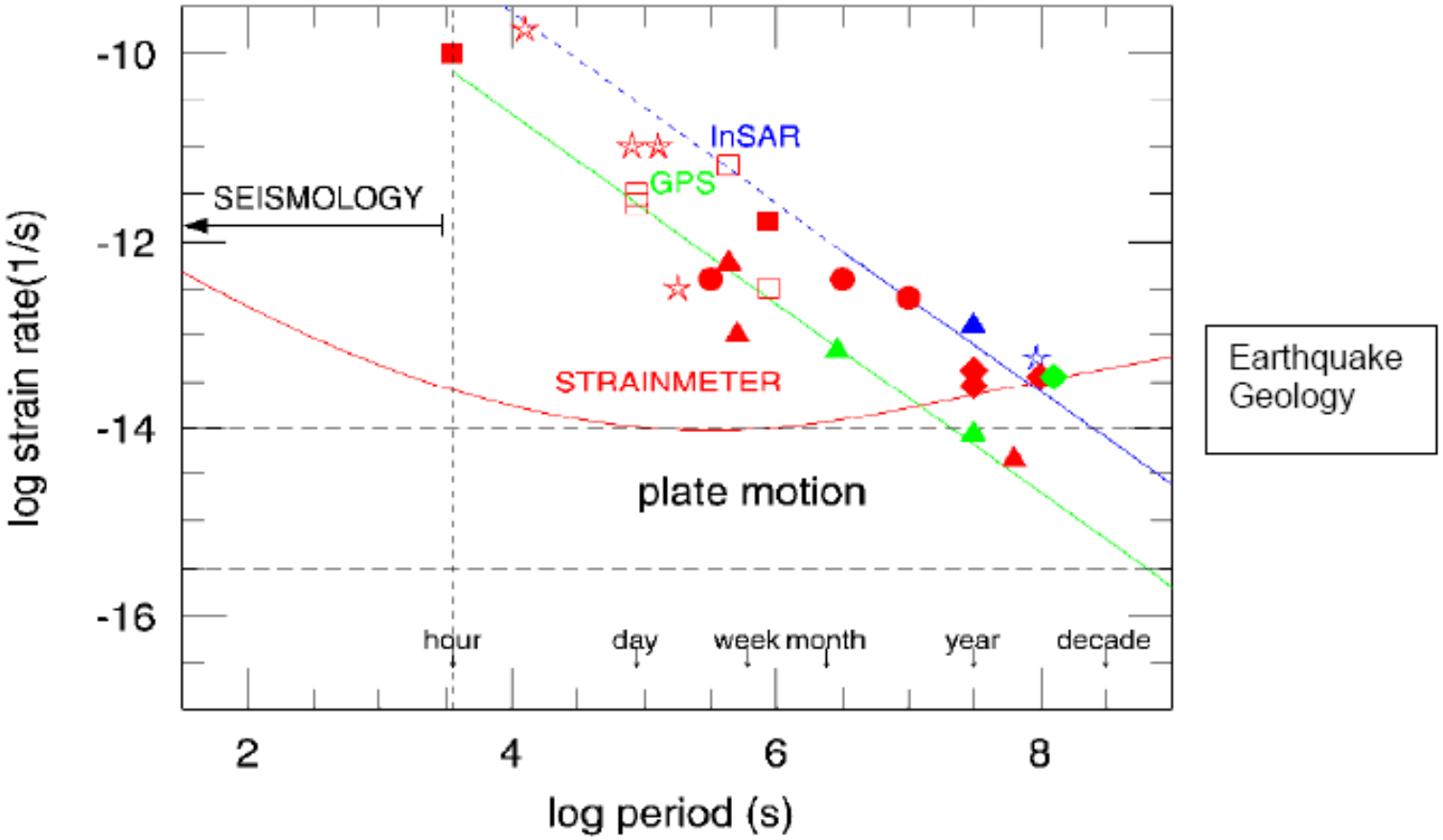

Space Geodetic Method

Overview of Space Geodetic Positioning Methods

Very Long Baseline Interferometry (VLBI)

Range-Difference (1 cm precision) :

$$\Delta r_{ij}(t) = \Delta \tau_{ij}(t) \cdot c$$

$$\approx -(\underline{r}_j - \underline{r}_i)_I \cdot \underline{s}_I = -\underline{b}_I \cdot \underline{s}_I$$

$$\approx -P\ N\ S\ W\ \underline{b}_{EF} \cdot \underline{s}_I$$

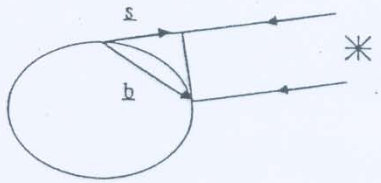

Satellite Laser Ranging (SLR)

Two-Way Range (1 cm precision) :

$$2 \cdot r(t) = \tau(t) \cdot c$$

$$\approx |[\underline{s}(t) - \underline{r}(t)]_I|$$

$$\approx |\underline{s}(t)_I - P\ N\ S\ W\ \underline{r}(t)_{EF}|$$

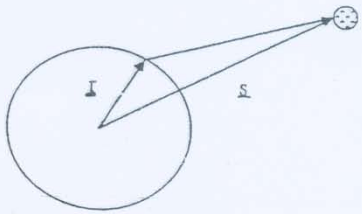

Global Positioning System (GPS)

Biased One-Way Range :

$$r(t) + n \cdot \lambda = \phi(t) \cdot \lambda = \tau(t) \cdot c + n \cdot \lambda$$

$$\approx |[\underline{s}(t) - \underline{r}(t)]_I| + n \cdot \lambda$$

$$\approx |\underline{s}(t)_I - P\ N\ S\ W\ \underline{r}(t)_{EF}| + n \cdot \lambda$$

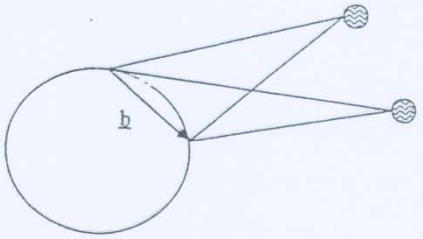

Double-range-differences (1-2 mm precision) : $\Delta^2 r(t) = \Delta^2 \tau(t) \cdot c$

VLBI

provide the coordinate on Earth

3.1(

VERY LONG BASELINE INTERFEROMETRY

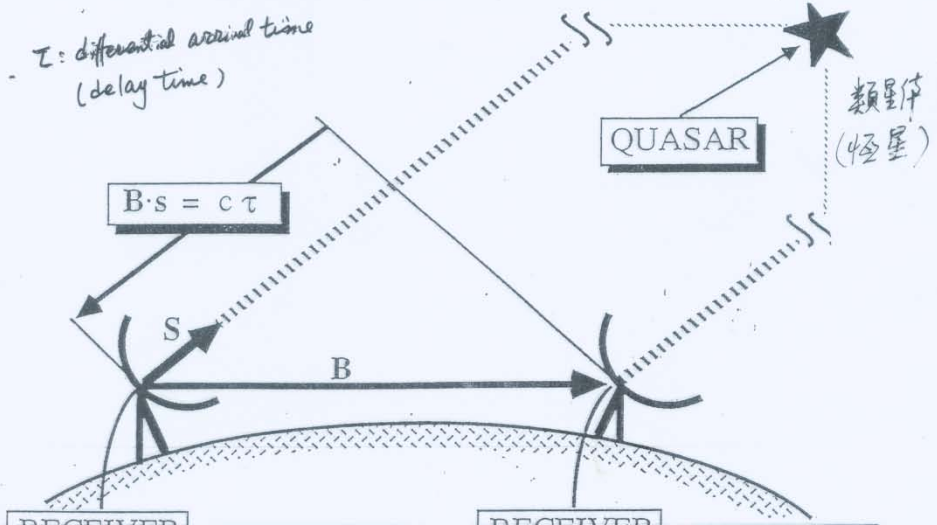

dual freq.

2.3 & 8.4 GHz

remove ionospheric effect

Troposphere is calibrated by meteorological measurements

GPS架構

- 太空衛星部份
- 地面監控部份
- 使用者部份

衛 星

24+3 衛星
周期11時58分
高度20,200公里

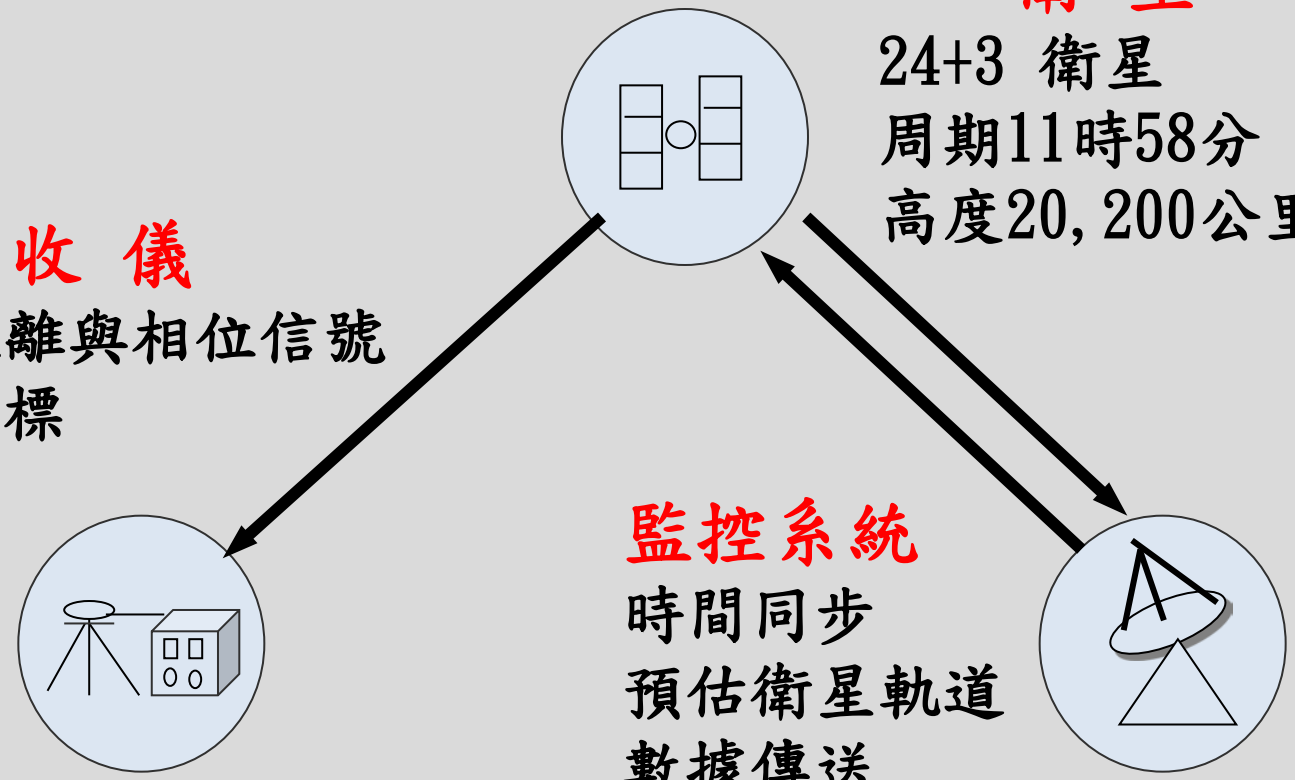

接 收 儀

接收虛擬距離與相位信號
接收衛星坐標
定位計算

監控系統

時間同步
預估衛星軌道
數據傳送
衛星狀況監測

GPS衛星分佈圖

Block I

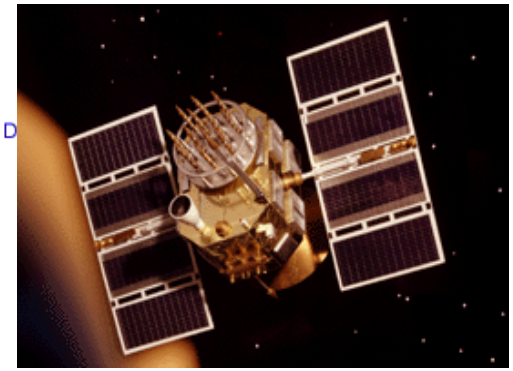

Block II

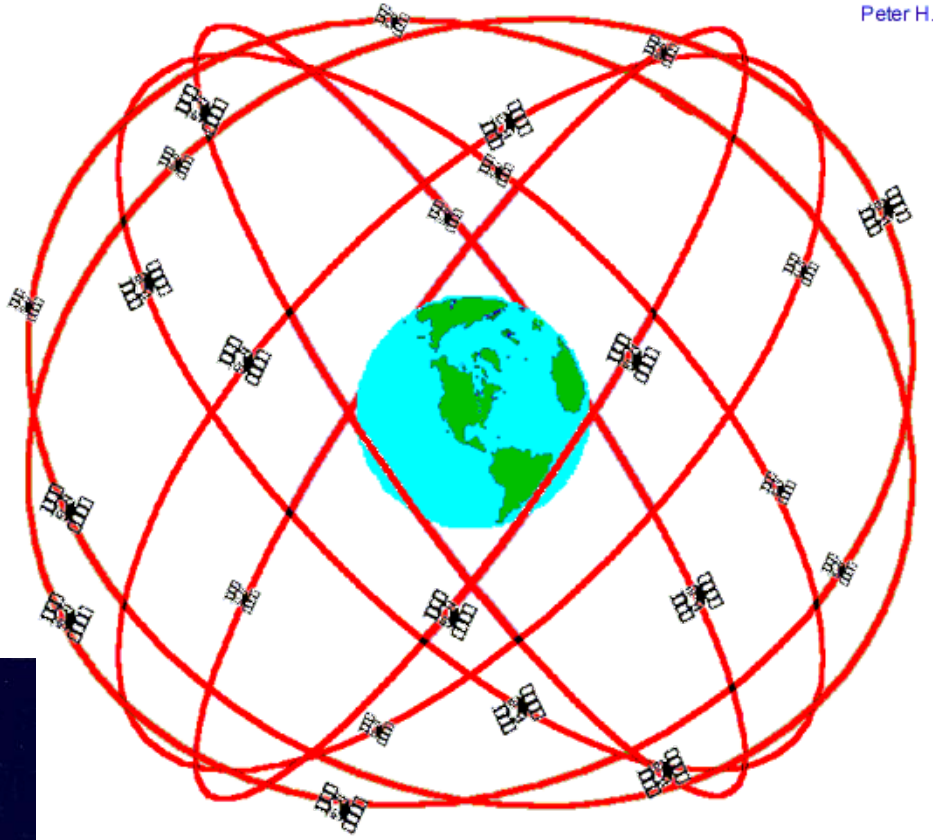

GPS Nominal Constellation
24 Satellites in 6 Orbital Planes
4 Satellites in each Plane
20,200 km Altitudes, 55 Degree Inclination

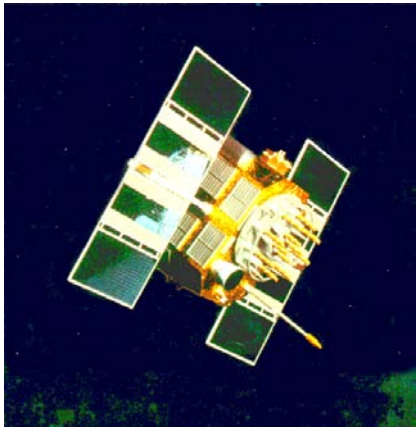

SV III

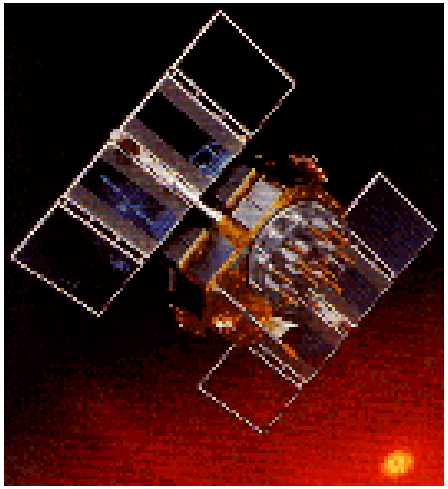

Block IIR

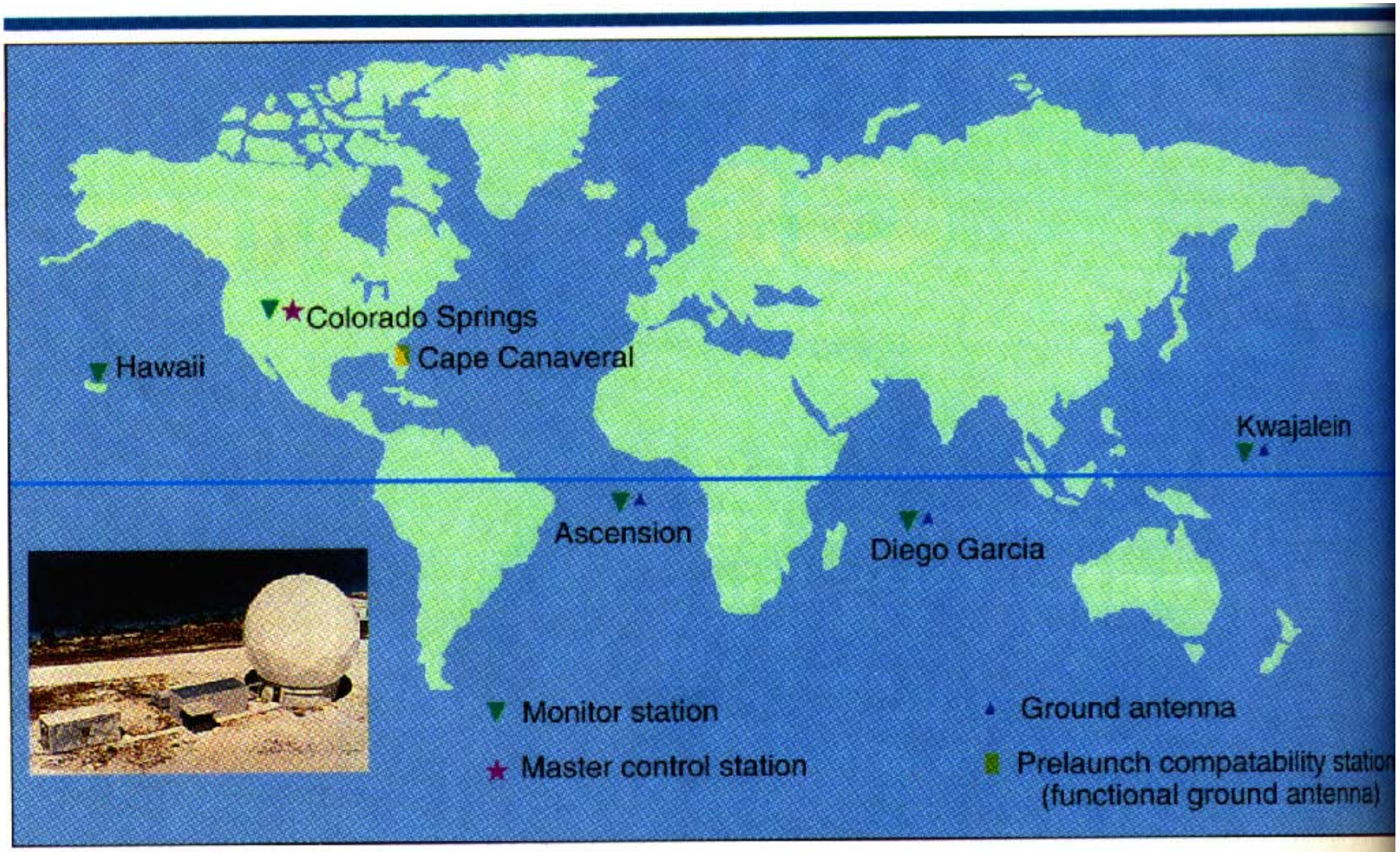

Figure 1. The GPS monitor stations and ground antennas, located worldwide, are the ears and eyes into the constellation. The inset photo is of Diego Garcia. Photo courtesy of the U.S. Air Force.

INSIDE GPS: THE MASTER CONTROL STATION

GPS訊號結構

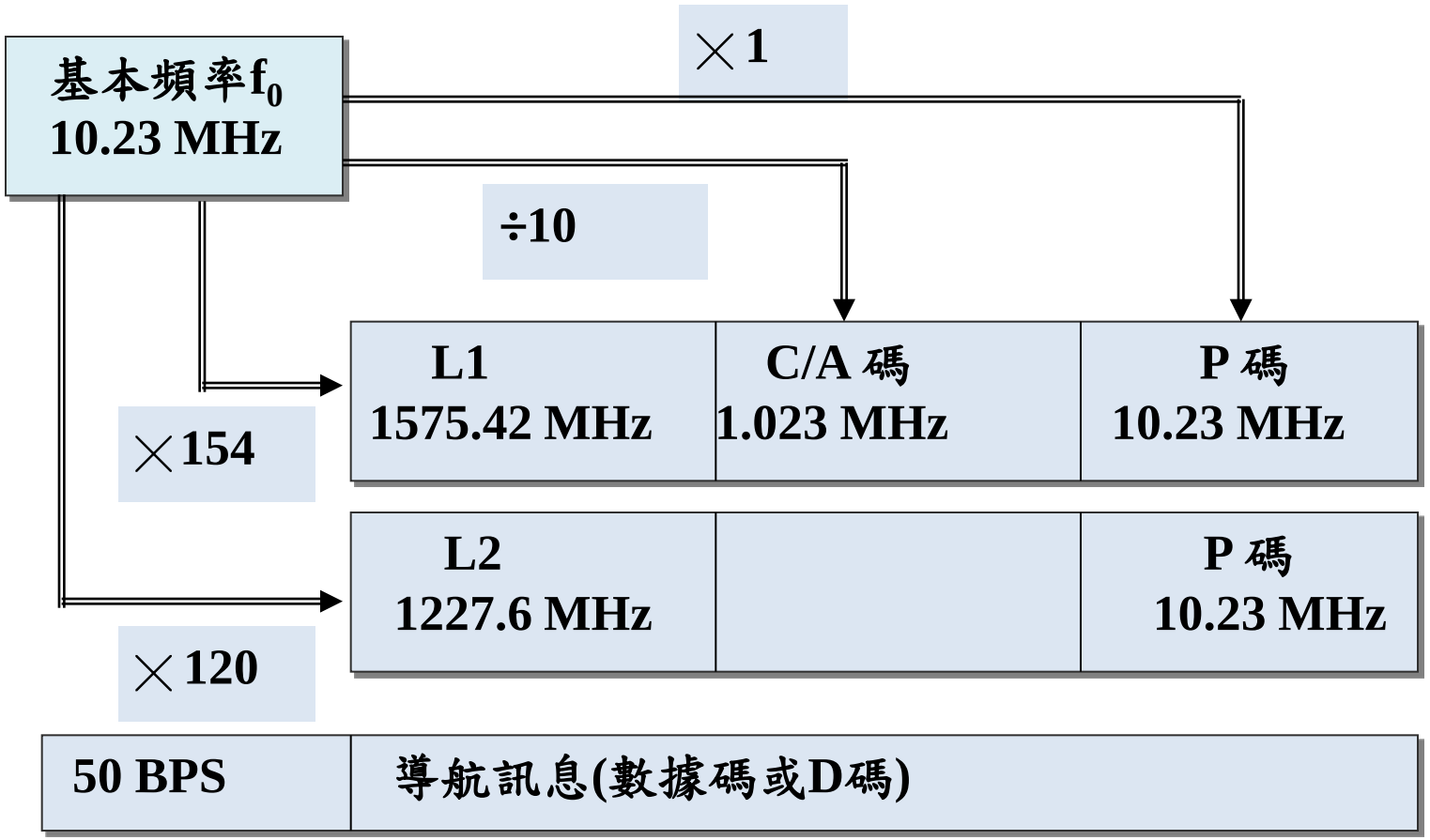
基本頻率f_0
10.23 MHz
×1
÷10
×154
×120
L1
1575.42 MHz
C/A 碼
1.023 MHz
P 碼
10.23 MHz
L2
1227.6 MHz
P 碼
10.23 MHz
50 BPS
導航訊息(數據碼或D碼)

GPS大地測量型接收儀

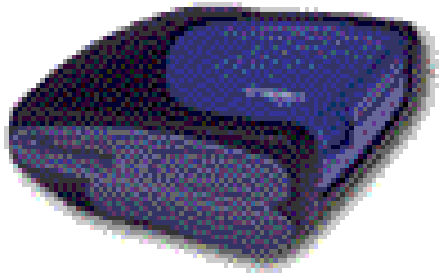

GPS導航接收儀


MAGELLAN


EAGLE
Explorer


GPSMAP 210
GARMIN


GPSMAP 220
GARMIN


Randon Antenna (spiral helix 錐形)

GPS定位精度

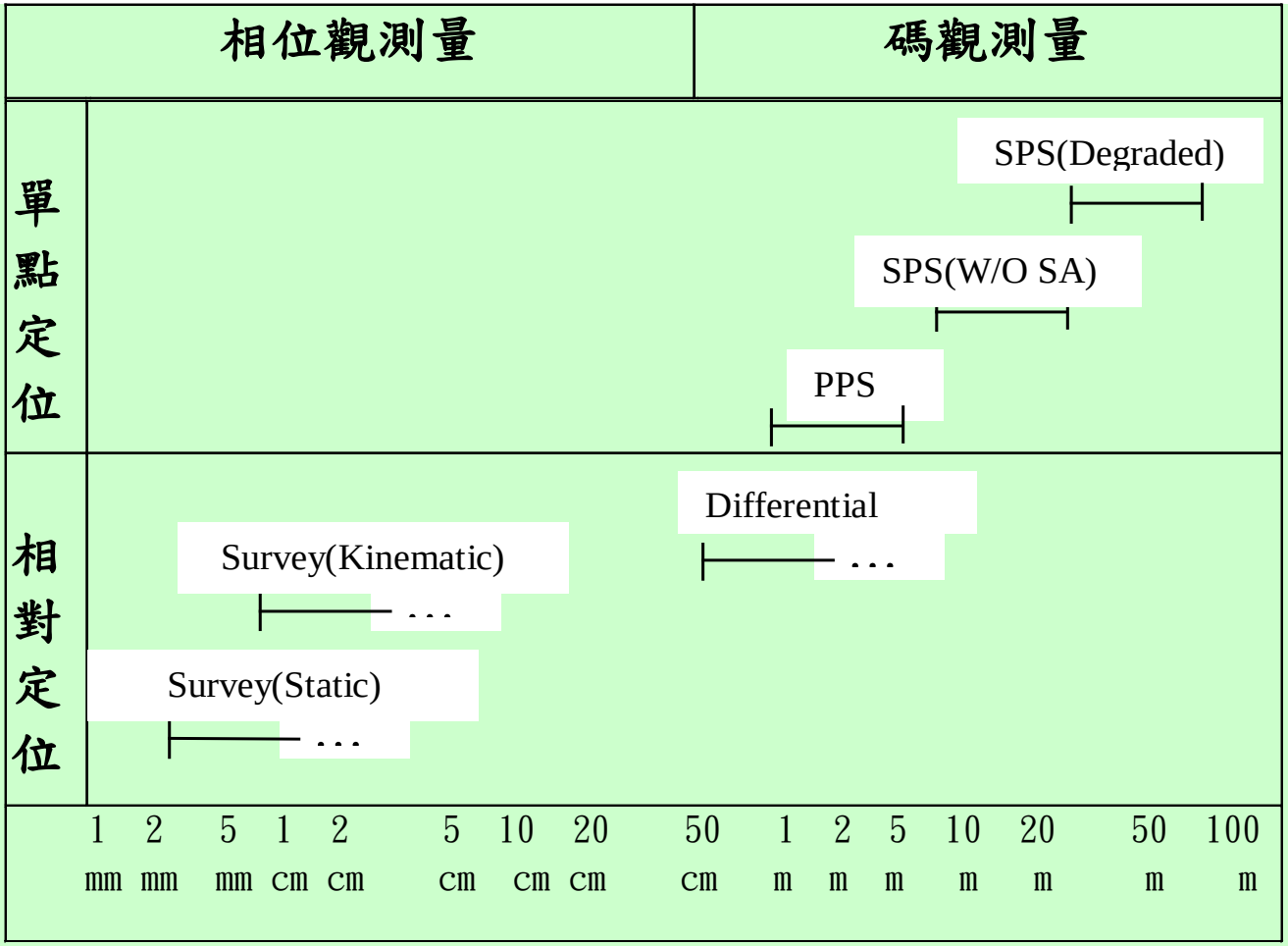

SPS--Standard Positioning Service(標準定位服務)

PPS--Precise Positioning Service(精密定位服務)

SA --Selective Availability (美國柯林頓總統決定於2000年5月2日起去除SA效應)

Global Continuous GPS Tracking Stations - IGS

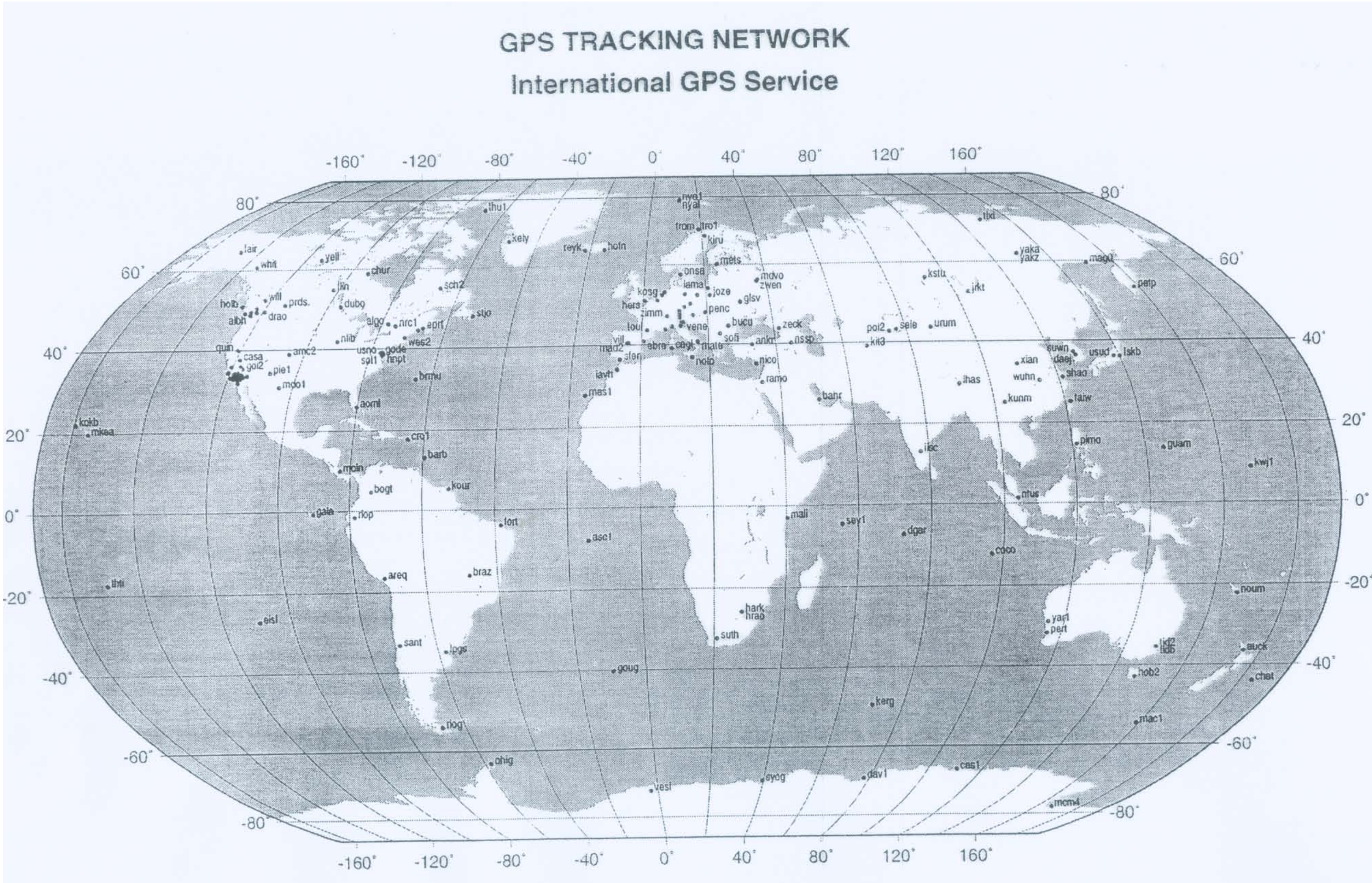

1993-1999 年各測點相對於澎湖白沙（S01R）之地殼水平運動速度分布情形，箭頭為測點之速度，星形為集集地震之震央，粗線為地表破裂帶及活斷層。顯示台灣地區在大地應力作用下，各地呈現不同的地殼運動型態

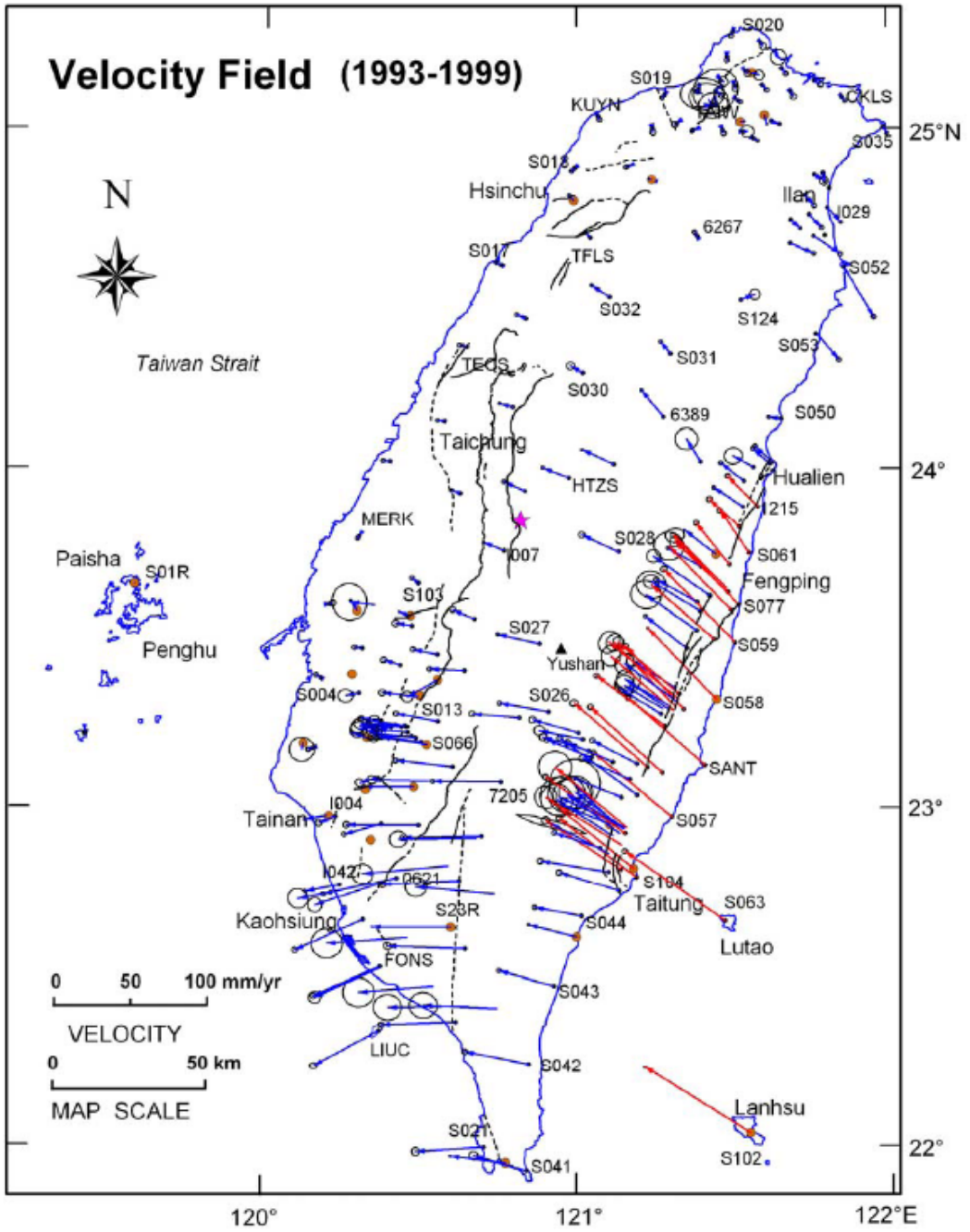

台灣GPS 衛星連續觀測網，藍方點為原有測站，紅圓點為2001-2004 年新設測站，黑三角形為預定站址，星形為其他機構新設或預定站址

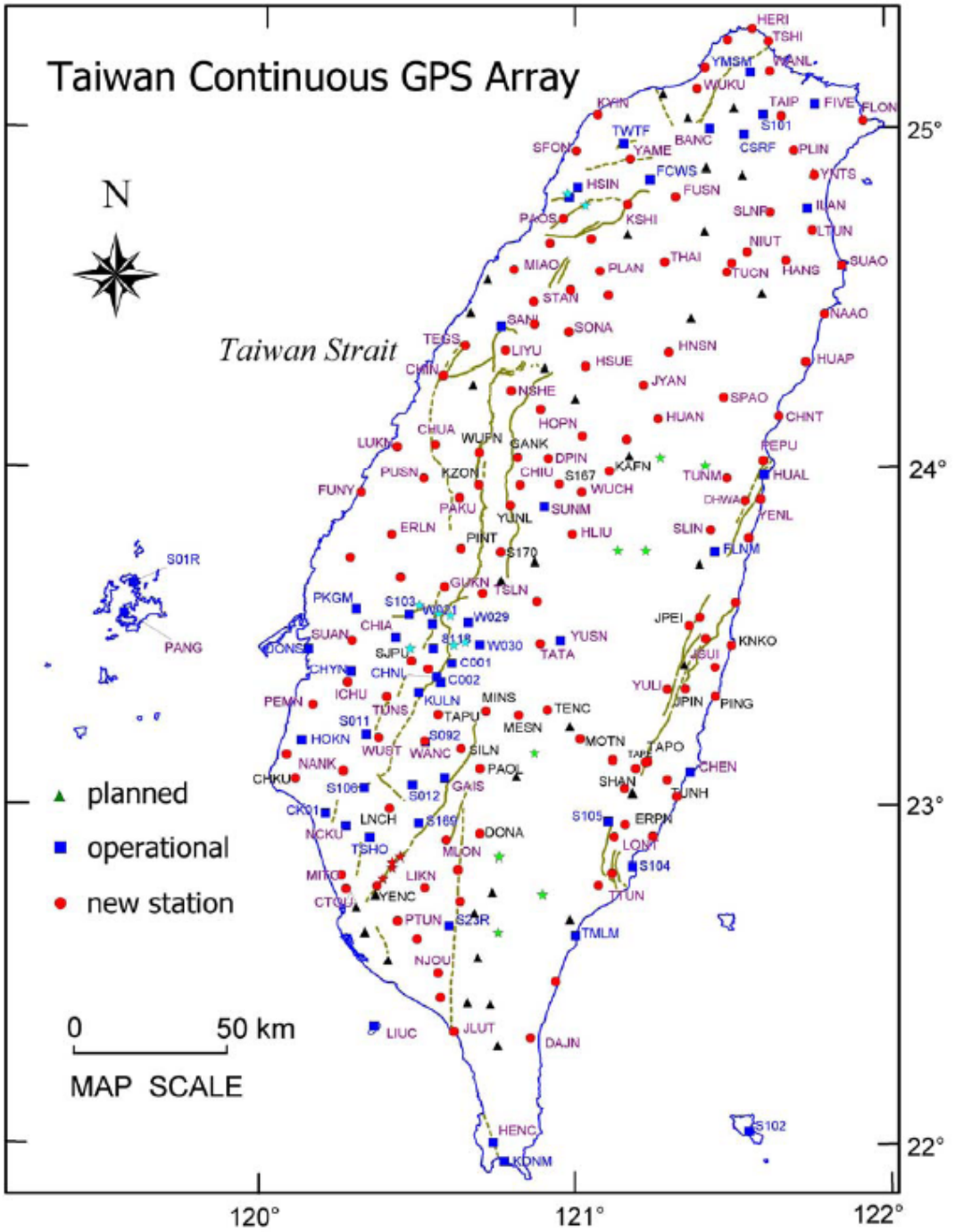

快速變形的區域

- 蘭嶼相對於澎湖每年8公分的縮短
- 海岸山脈兩邊(約10公里)每年2公分的縮短
- 過去已有地殼變動監測基礎
- 地震相對性的稀少

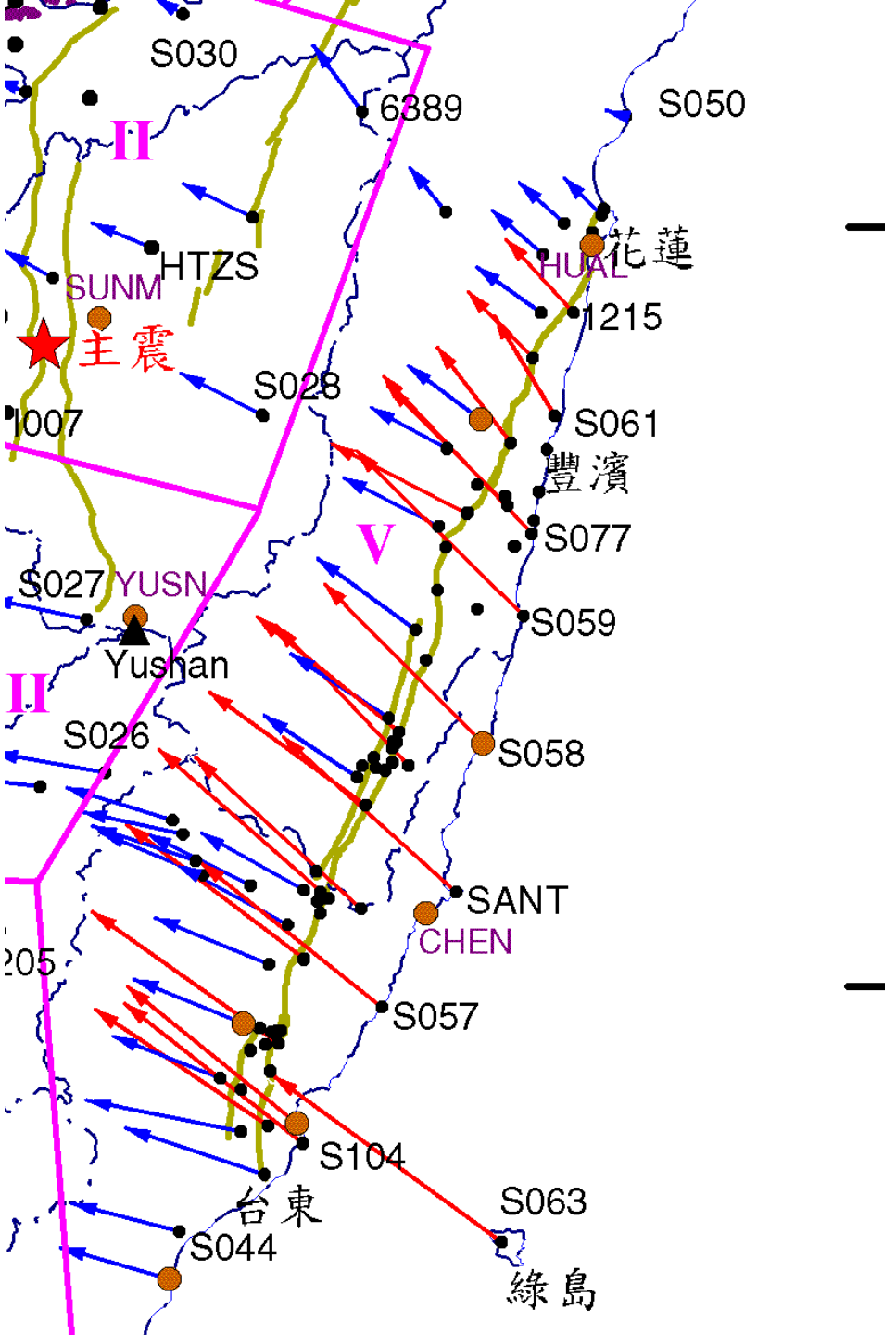

板塊邊界的移動速率

參考 地球所 郭隆晨 博士所設立的 GPS LAB 網站
http://gps.earth.sinica.edu.tw/images/ppt/horizontal_velocity_s01r_2007-2008.gif

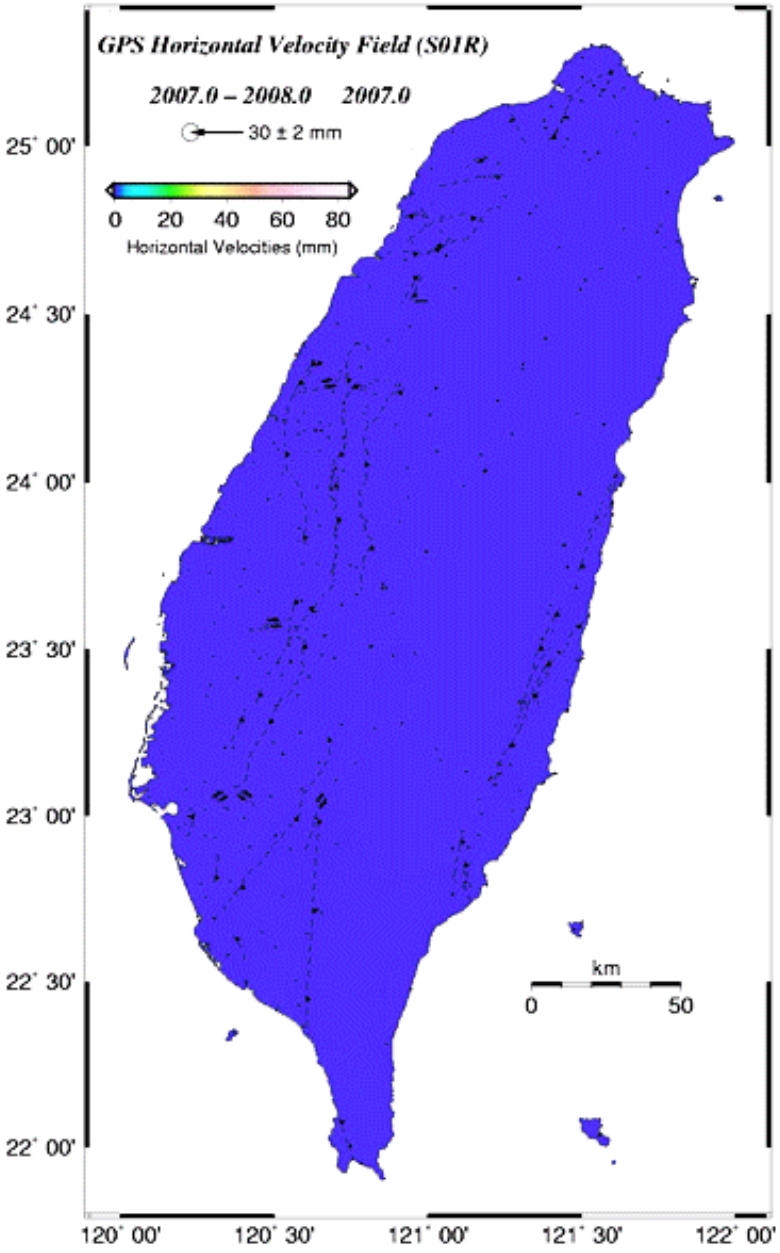

Rates of Erosion and Uplift

1. Determining rates of erosion.
   （計算侵蝕速率）
2. Calculating mass balances and material fluxes.
   （計算抬昇速率）
3. Determining rates of uplift.
   （計算物質進出和面積守恆）
4. Reconstructing the past geometry of tectonically active landscape.
   （重新建構過去地質構造活動的規模）

參考書: Tectonic Geomorphology, Burbank and Anderson, 2001, Ch. 7. Blackwell Pub.

岩盤抬昇、剝蝕、壓密及沈積作用交互影響地表地形

地表抬昇＝岩盤抬昇＋沈積-壓密-剝蝕

(surface uplift= bedrock uplift + deposition -compaction-denudation)

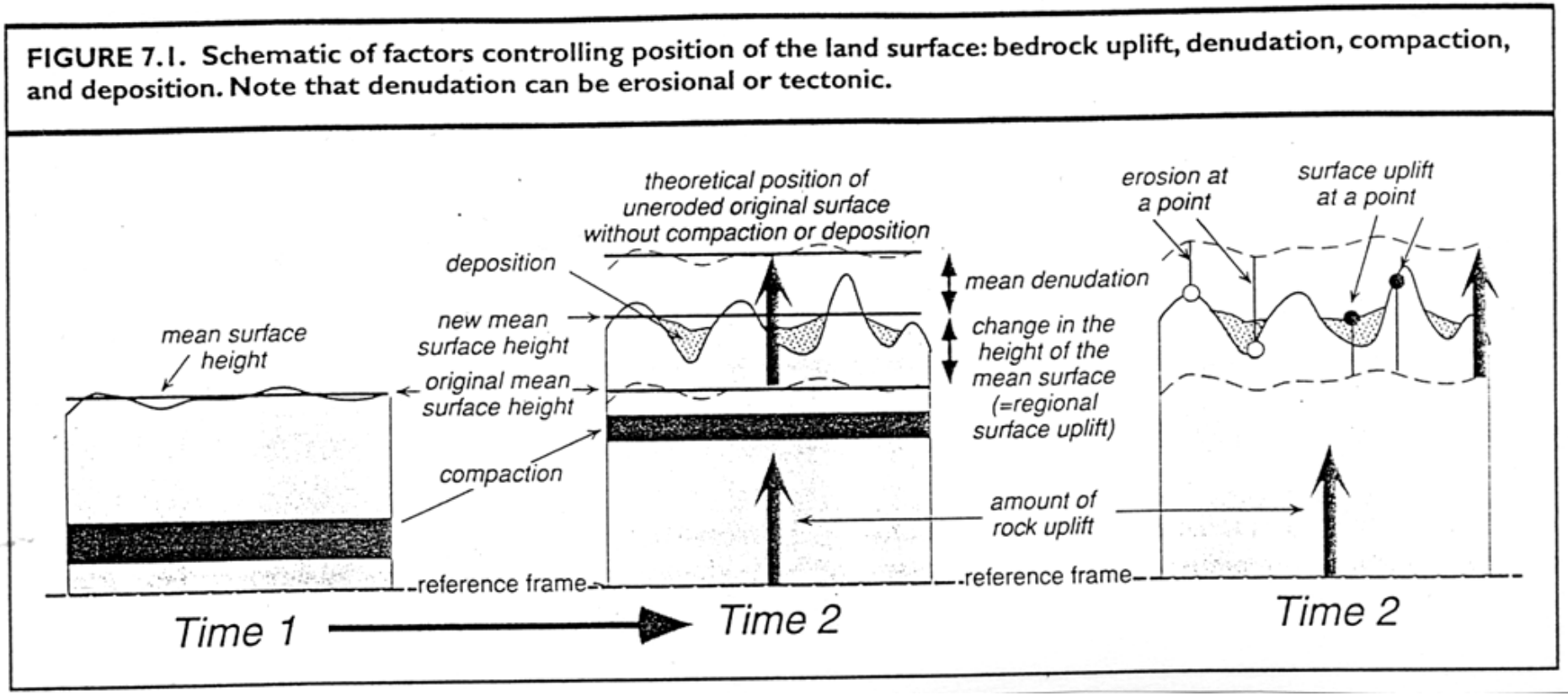

計算剝蝕速率的方法。

FIGURE 7.3. Approaches to estimating denudation rates

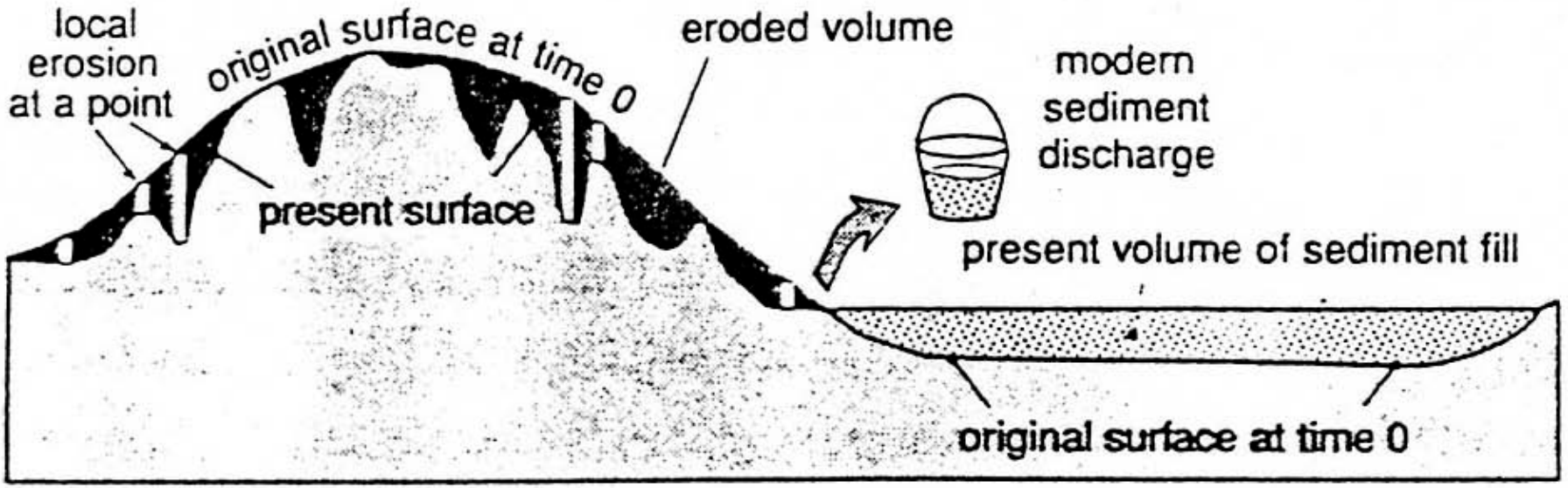

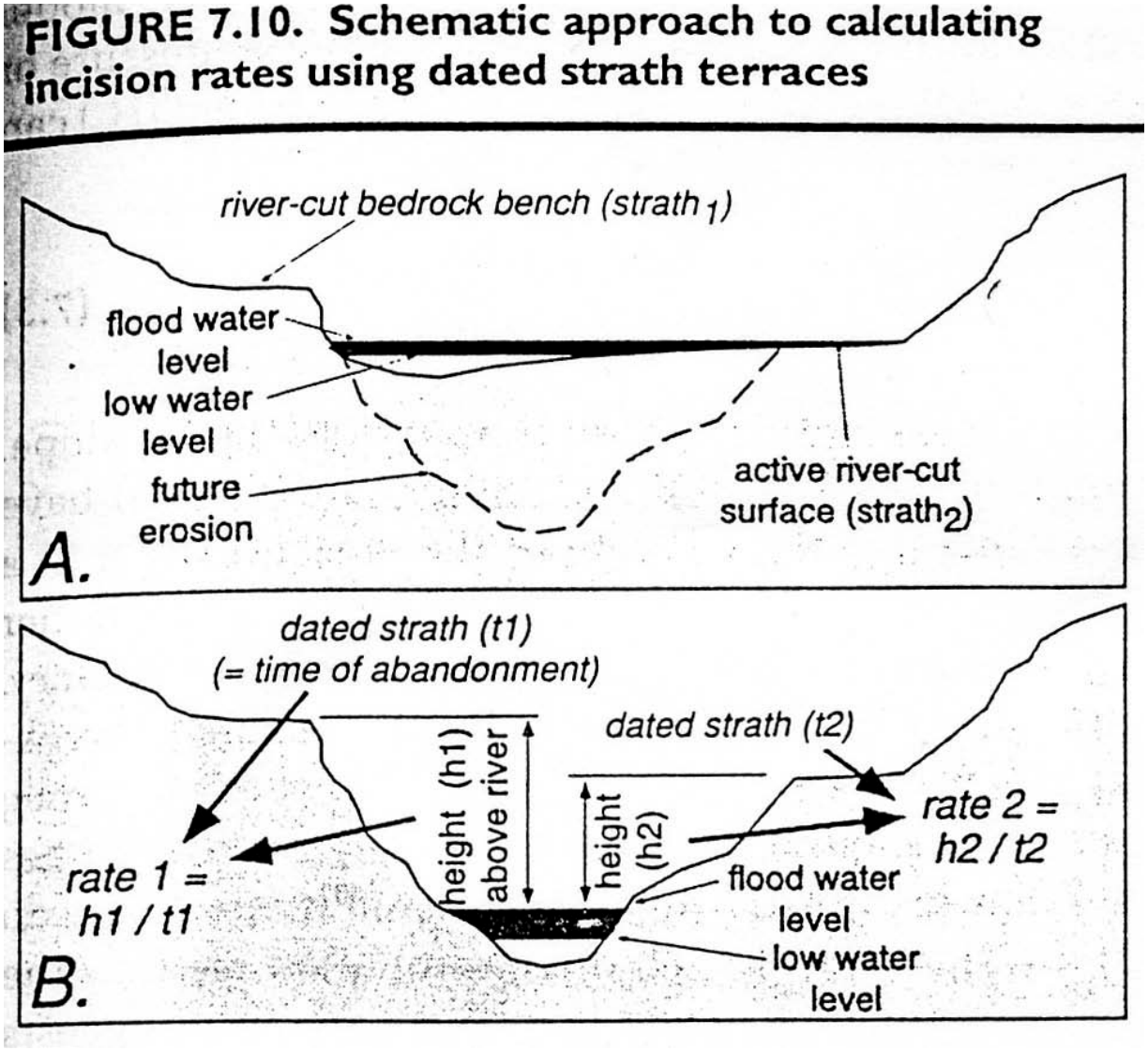

利用河階台地計算下切速率。

由放射性定年計算長期侵蝕速率

地殼岩石冷卻因素：

1. 熱調節～岩漿、熱液或變質事件
2. 岩石被移近地表–
   構造運動或侵蝕作用

在岩石冷卻的過程中，對不同放射性定年系統的特定礦物必定會歷經其封存溫度

Apatite Fission Track

Mean track lengths are ca. 14-15 µm.

Cooling, Burial Paths

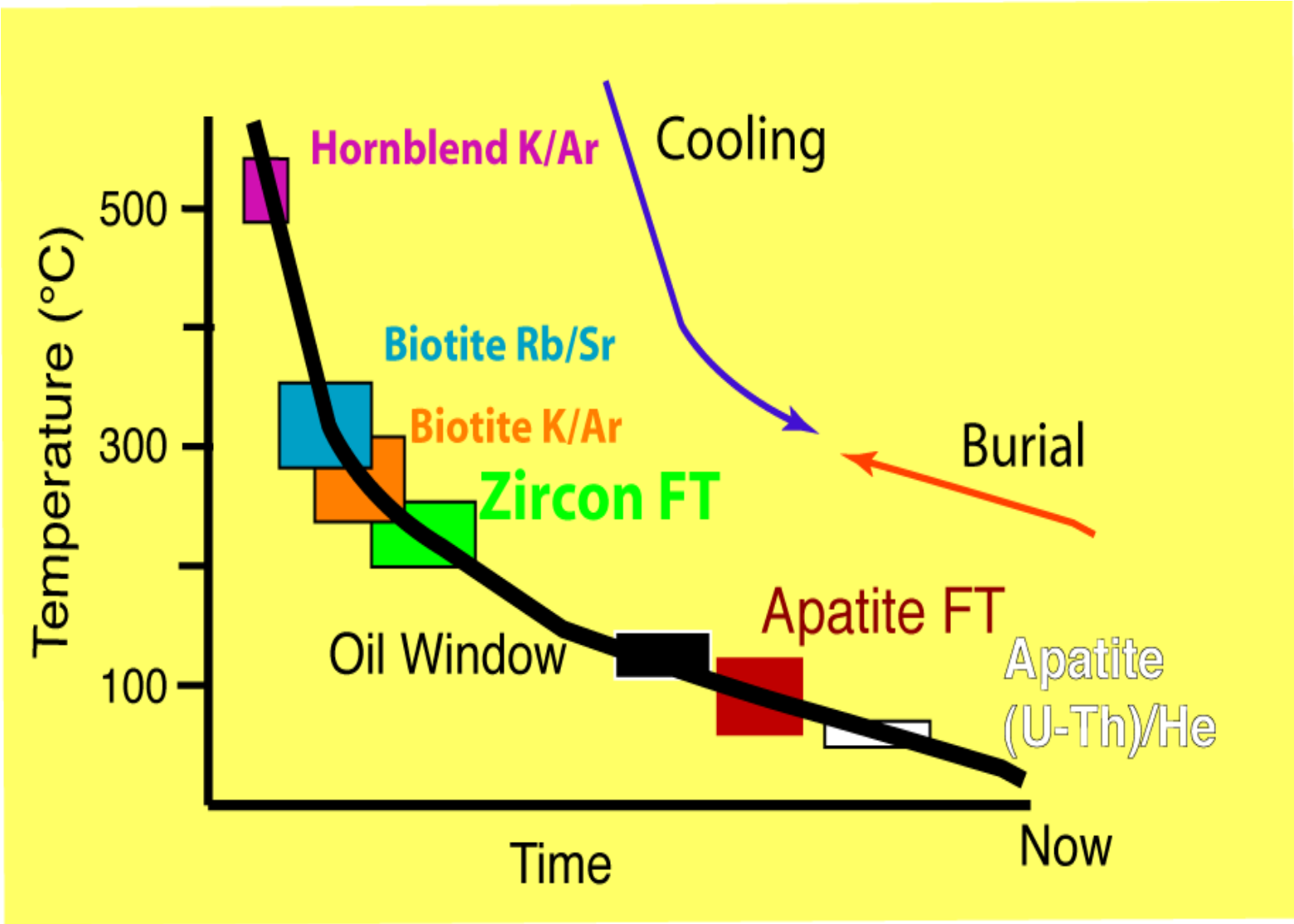

Radiometric dating systems and closure temperature for some minerals

Mineral and sating system	Closure temperature
Hornblende (K-Ar)	525±25°C
Muscovite (K-Ar)	325±25°C
Biotite (K-Ar)	300±25°C
K-feldspar (K-Ar)	200±25°C
Muscovite (Rb-Sr)	500±25°C
Biotite (Rb-Sr)	275±25°C
Monazite (U-Pb)	525±25°C
Sphene (fission track)	275±25°C
Zircon (fission track)	225±15°C
Apatite (fission track)	120 ±20°C

FIGURE 7.14. Cartoon of contrasting cooling histories derived from ^{39}Ar-^{40}Ar dates on hornblende, muscovite, and potassium feldspar on two different rock samples

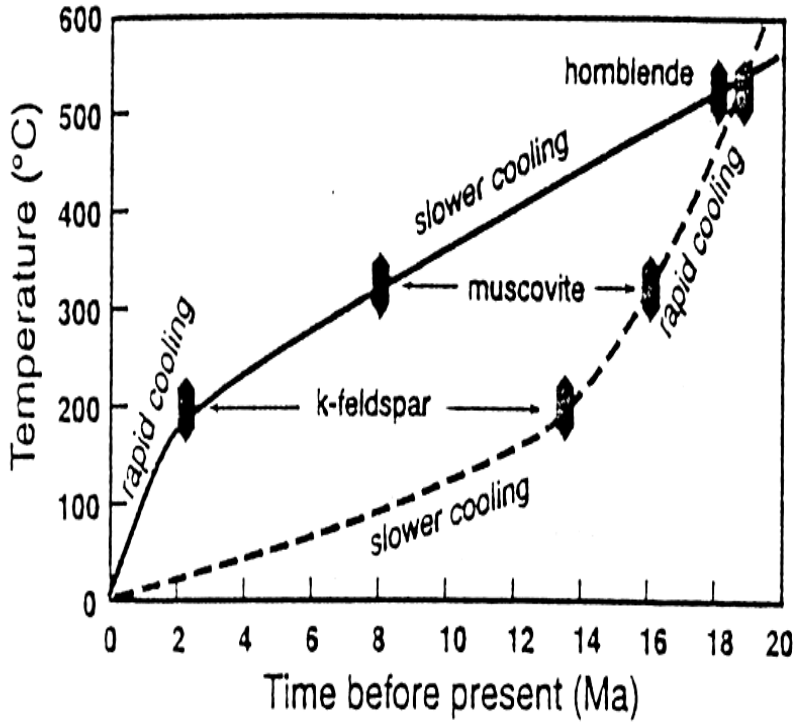

Cooling rate

Rapid cooling 100 ℃/ My

Slower cooling 1~20 ℃/ My

由於冷卻作用會持續到現今，所以常用來推論剝蝕速率的增快，例如：對現今的正斷層而言，表面侵蝕增快造成冷卻速率變快。綜合侵蝕和冷卻速率時，必須考慮地溫梯度，一般以20-30℃/Km為地殼的地溫梯度。

結合侵蝕速率和冷卻速率

$z = c/(dT/dz)$　　z：深度

c：封存溫度

dT/dz：地溫梯度

$E = z/a$　　E：侵蝕速率

a：封存溫度的間隔時間

以上圖rapid cooling為例：當岩石溫度降到200℃以下，約花了2Ma，以20-30℃ /Km為地殼的地溫梯度換算的到3～5Km/My (3-5 mm/yr) 的剝蝕速率。

（Uncertainty: 古地溫梯度）

Apatite Fission Tracks

- Above 60°C, tracks accumulate over geologic time
- Between 110 and 60°C, not all tracks are annealed
- Below 110°, fission tracks are annealed (healed up and removed) quickly

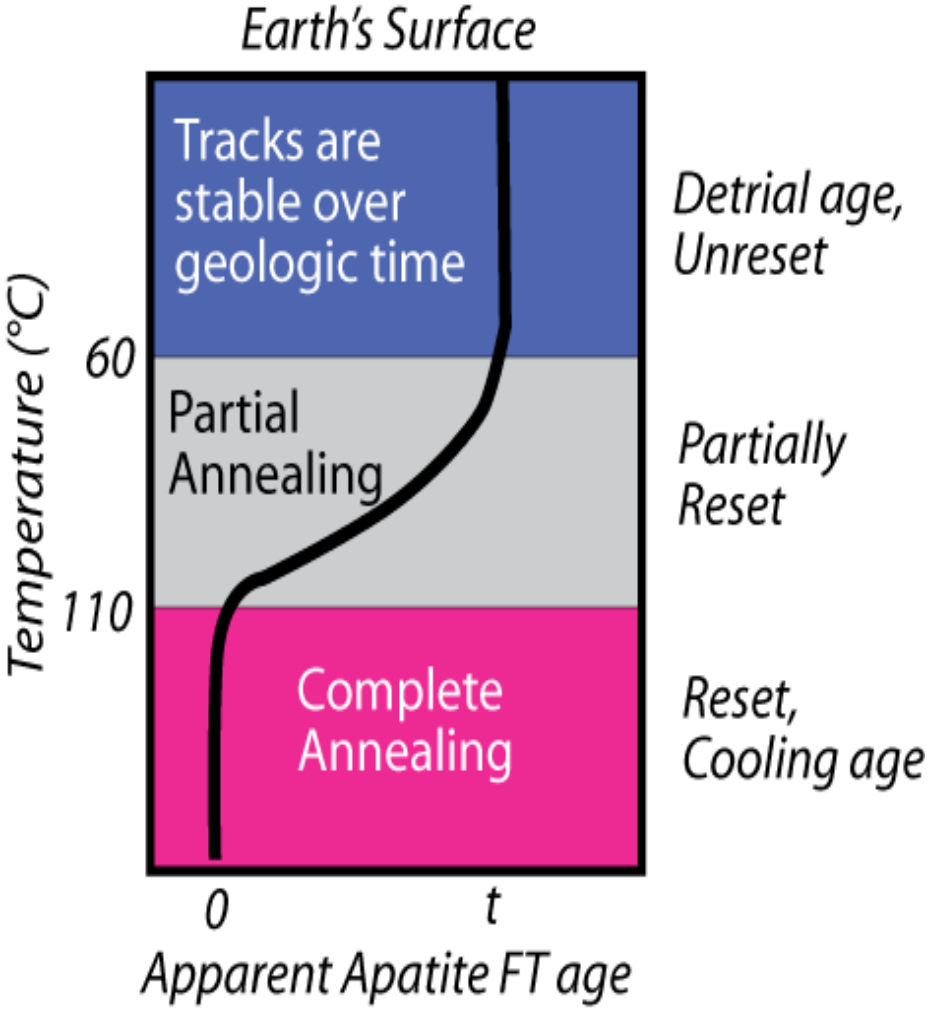

Interpretation of Fission Track Ages

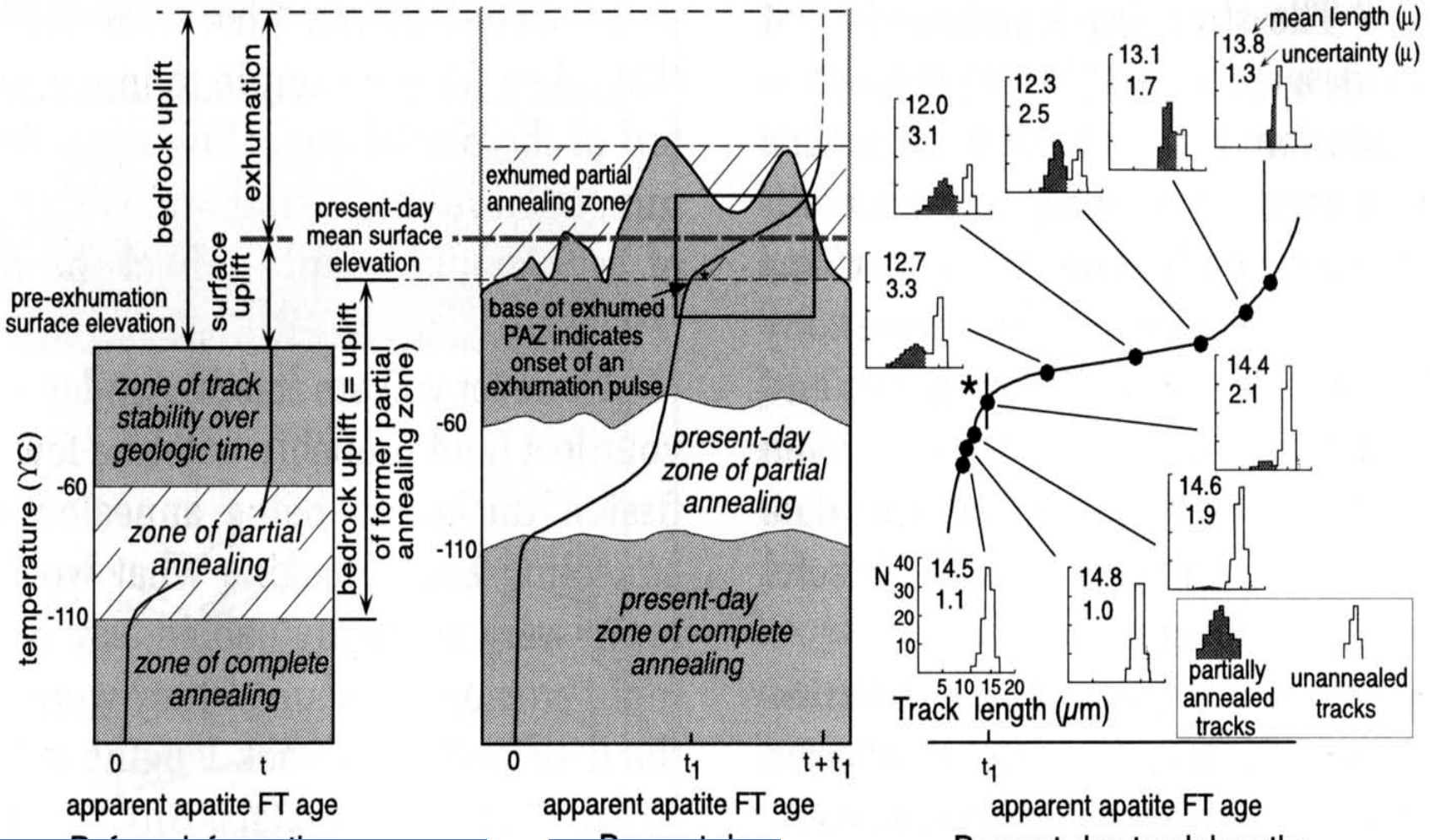

Before Deformation

Today

Observed Track Lengths

From: Burbank and Anderson (2001)

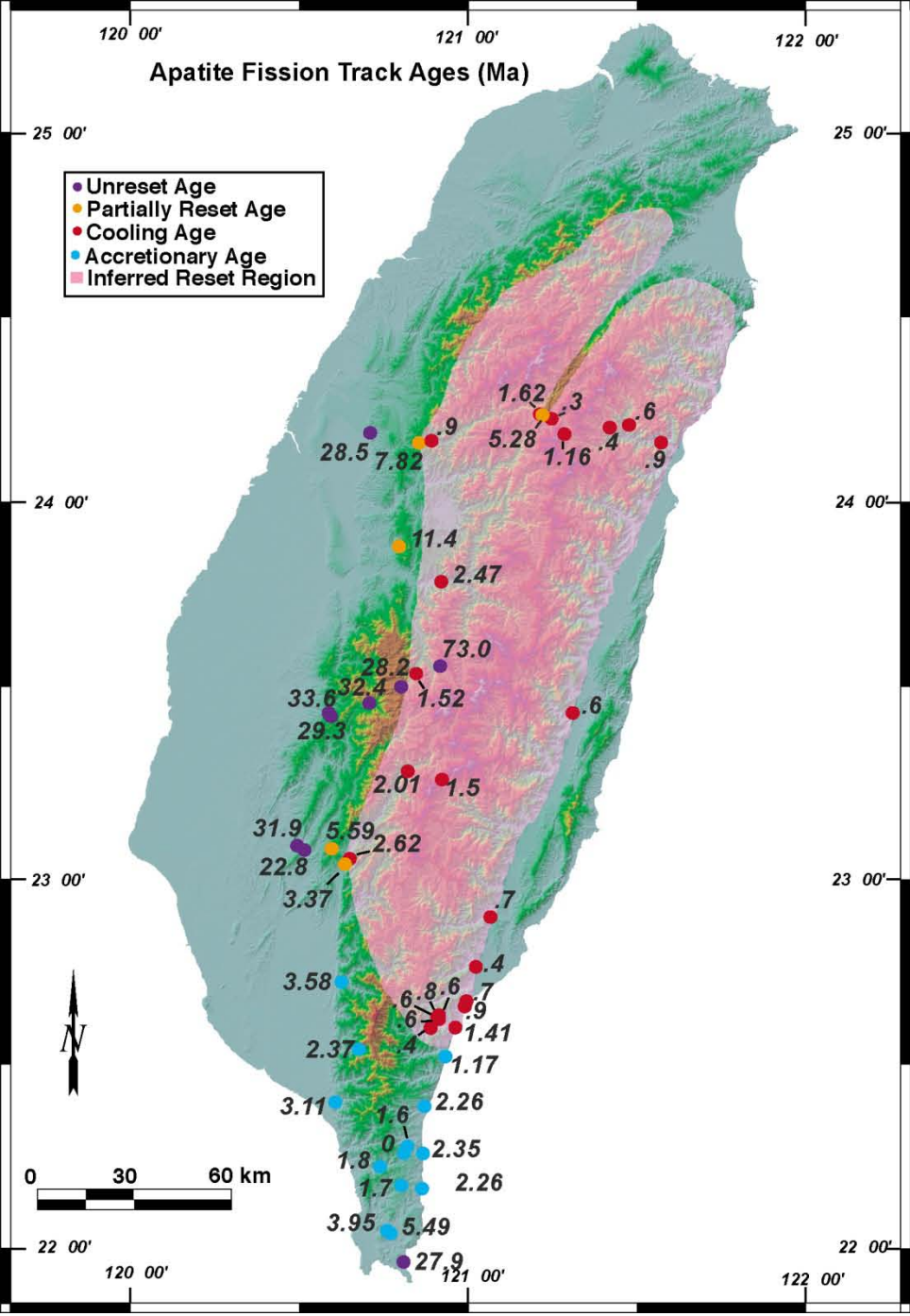

Locations and pooled age of AFT

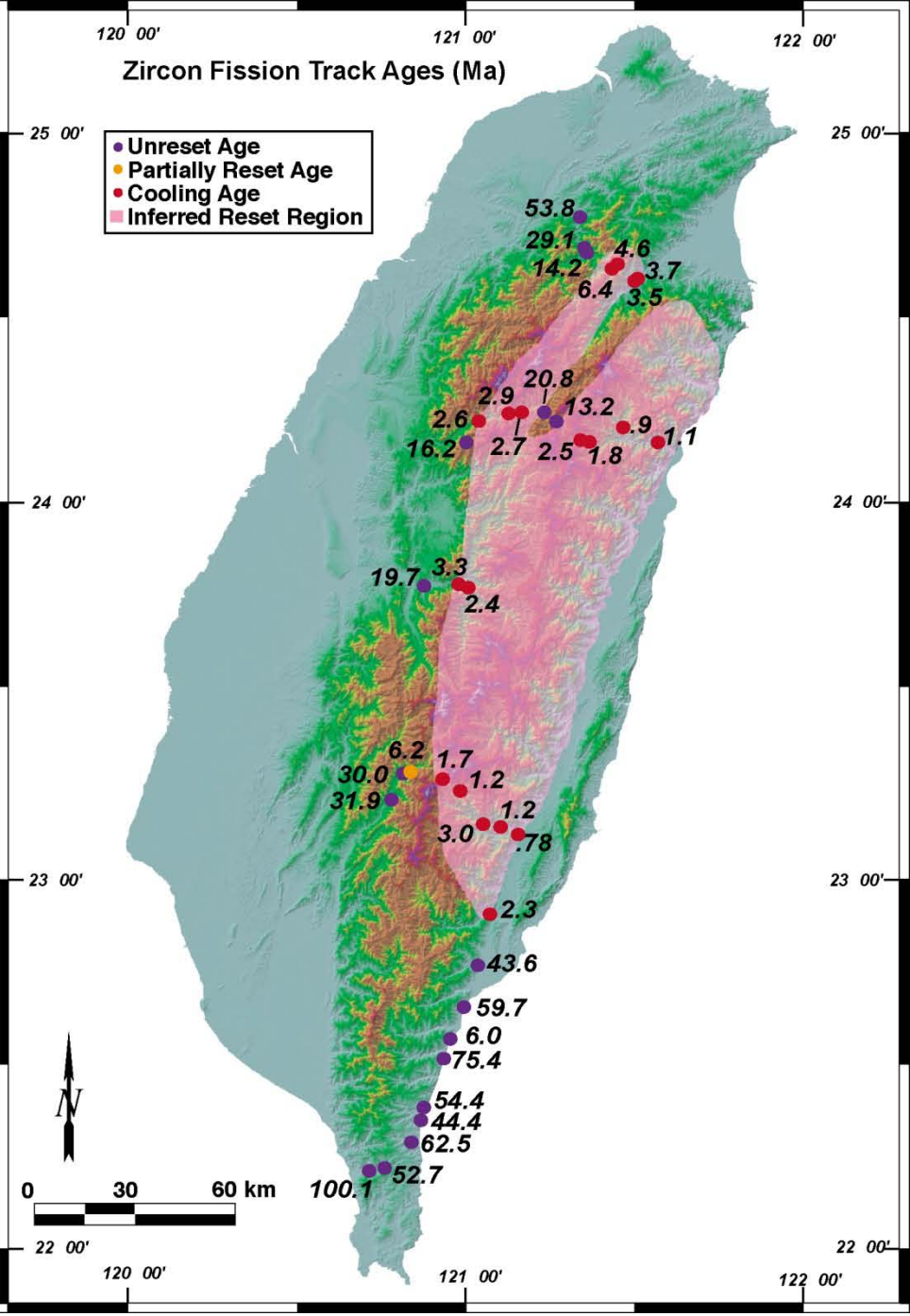

Locations and pooled age or χ^2 ages of ZFT

Characteristics of Fission Track Dating Results

1. Widths of the AFT and ZFT reset age zones remain nearly constant between 23^{o}~24^{o} (40 km wide) – steady state exhumation.
2. Southward propagate collision is consistent with reset ages in the north and unreset ages in the south.
3. Ongoing collision is also recorded in the difference of reset zones between AFT and ZFT.

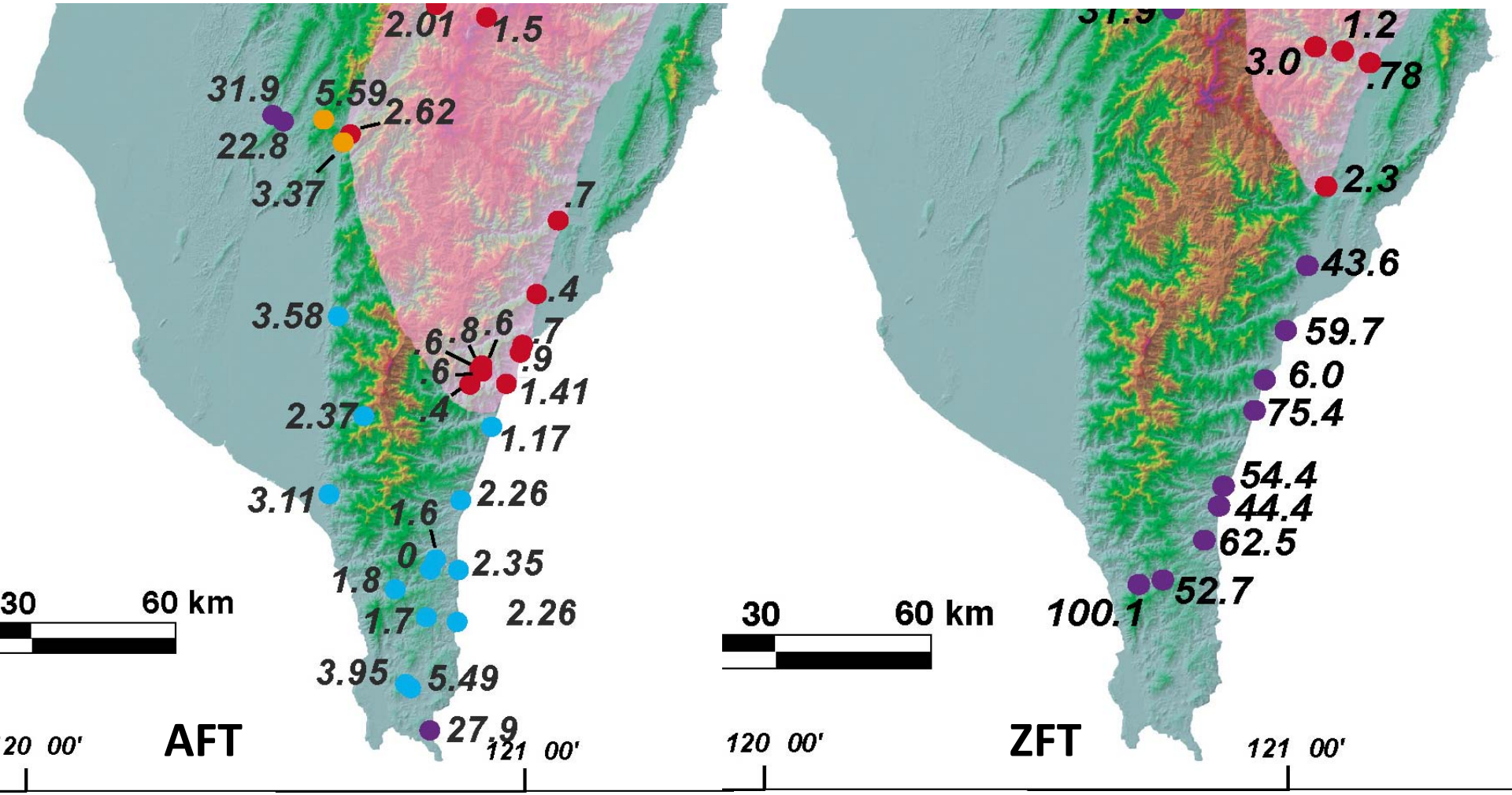

Southern Taiwan Ages: sediments reset by hot (high geothermal gradient) oceanic crust during burial

- Cooling by conduction with cold underthrust slab in accretionary wedge?
- Submarine erosion?
- Subaerial erosion starting at 2Ma?

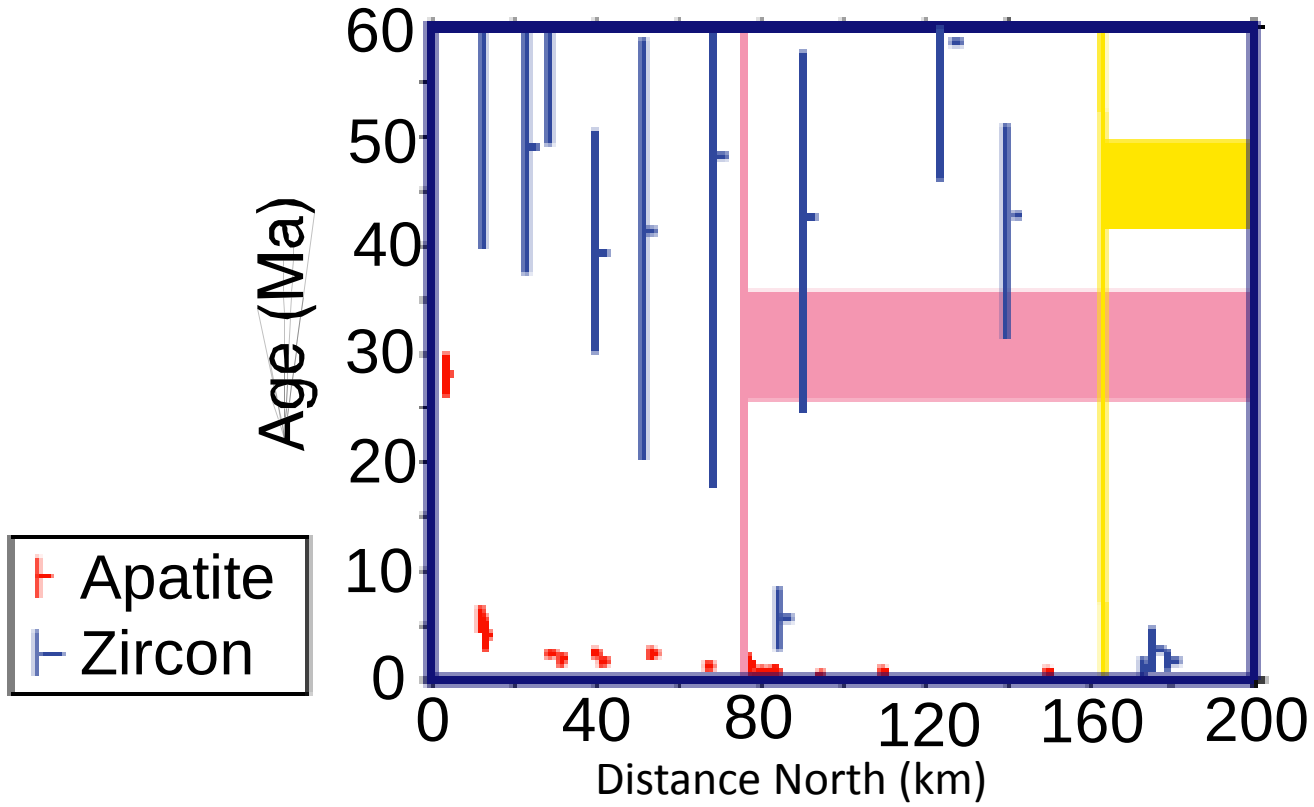
Age (Ma)
60
50
40
30
20
10
0
0
40
80
120
160
200
Distance North (km)
Apatite
Zircon

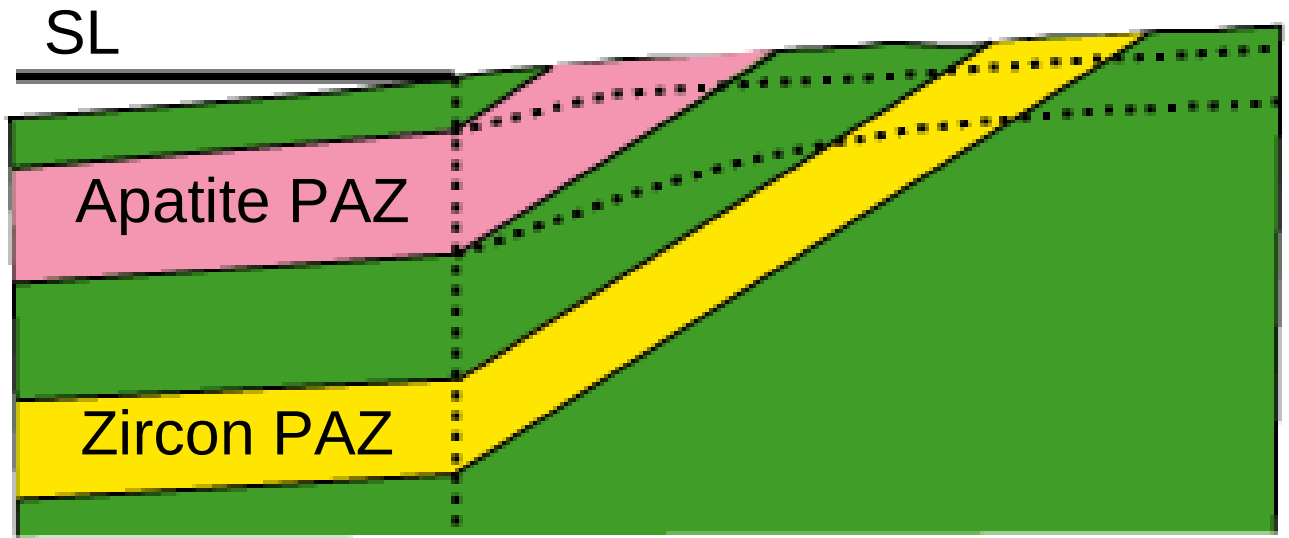
SL
Apatite PAZ
Zircon PAZ

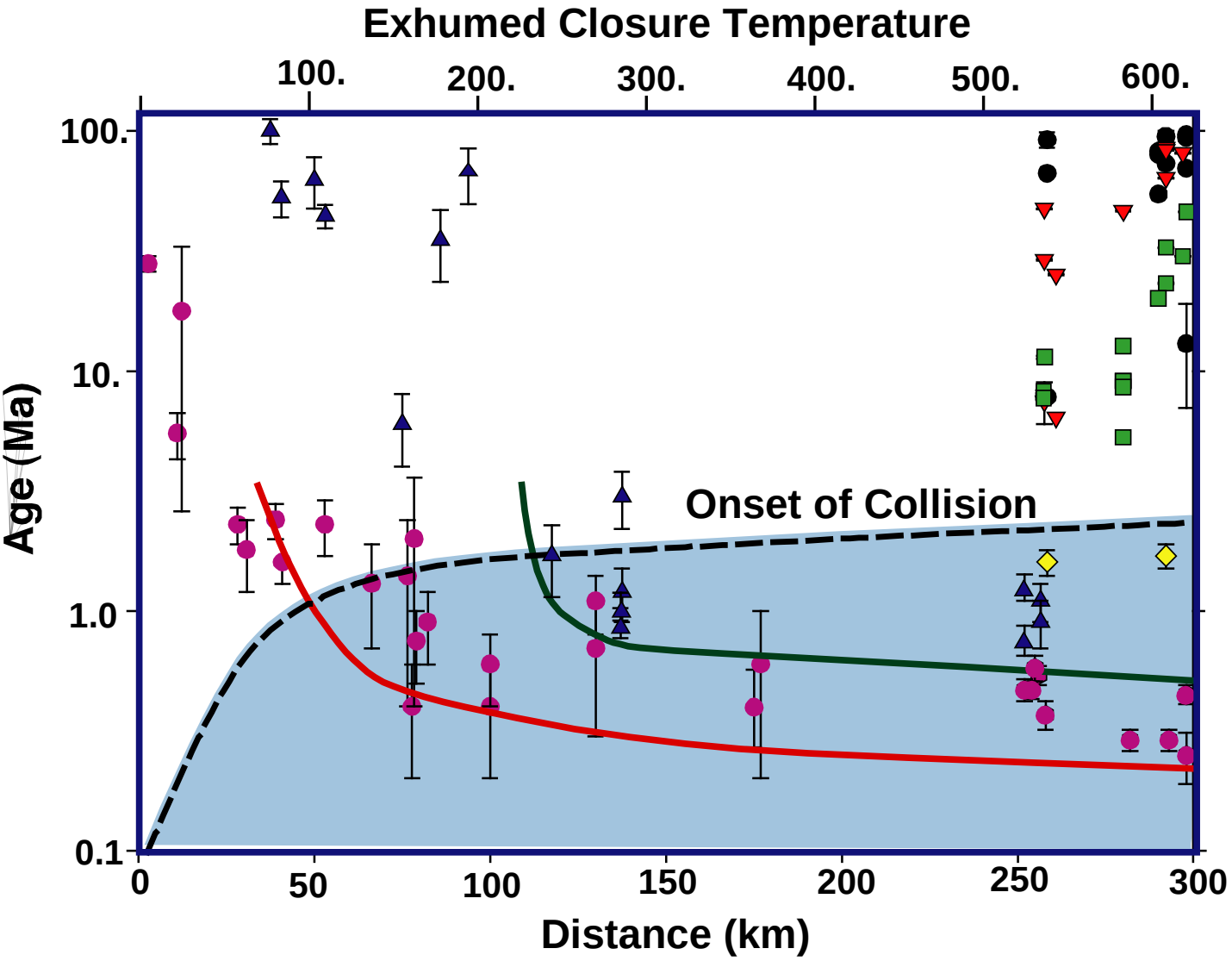

(Closure Temp °C)

- Ar/Ar Hb (680°)
- Ar/Ar Mus (350°)
- Ar/Ar Biot (350°)
- Ar/Ar Mcl (150°)
- ZFT (240°)
- AFT (100°)

1-D Thermal Model

$\dot{e}$ = 5 mm/yr

V_p = 60 mm/yr

$\left(\frac{dT}{dz}\right)_i$ = 25°C/km

- Apatite Age
- Zircon Age

Apatite and Zircon fission track ages as a function of distance from southern end of Taiwan

Best fit of erosion rate ~4-5 mm/yr

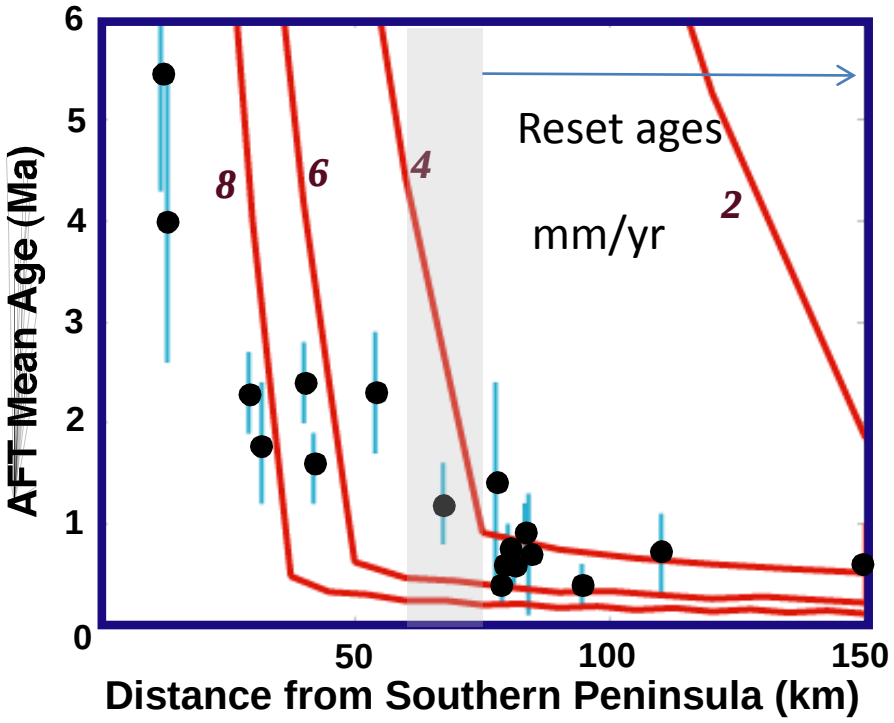

Best fit of erosion rate ~5-6 mm/yr

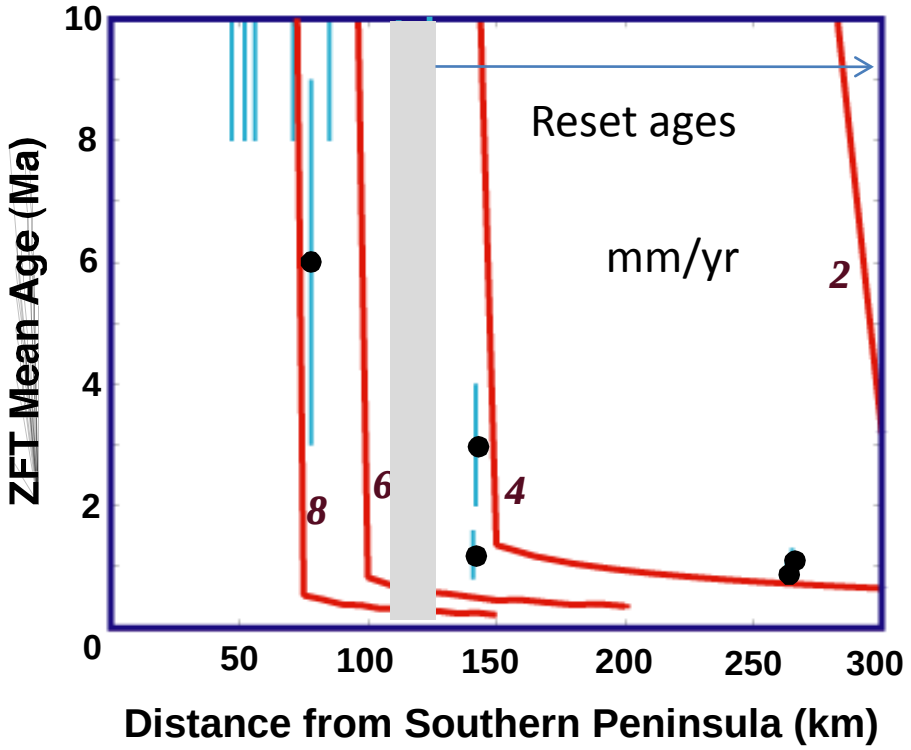

Parameters of 1-D thermal model see previous slide except various erosion rate

Note: Predicted reset ages become progressively younger with time or distance to the north
Transition from unrest to reset ages is very sensitive to the erosion rate

Western Taiwan FT and He Ages

20-01 UR
Tangenshan Fm
FTAge = 22.8(2.6) (F)
AHe = 1.8 Ma

23-01 R
Upper Changshan Fm
FTAge:3.4(-.6+.7)(P)
AHe Age: 1.3

17-01 UR
Ailiaochioa Fm
FTAge = 31.9 (2.4) (F)
YPA=15.1(-1.8+2.1)
AHe Age = 1.8 Ma

21-01 PR
Changchikeng Fm
FTAge = 5.6(.6) (F)
YPA=1.3(-.4+.5)
AHe Age = .4 Ma

24-01 PR
Lower Changshan F
FTAge =2.6(1.0) (P)
YPA:1.8(-.7+1.2)

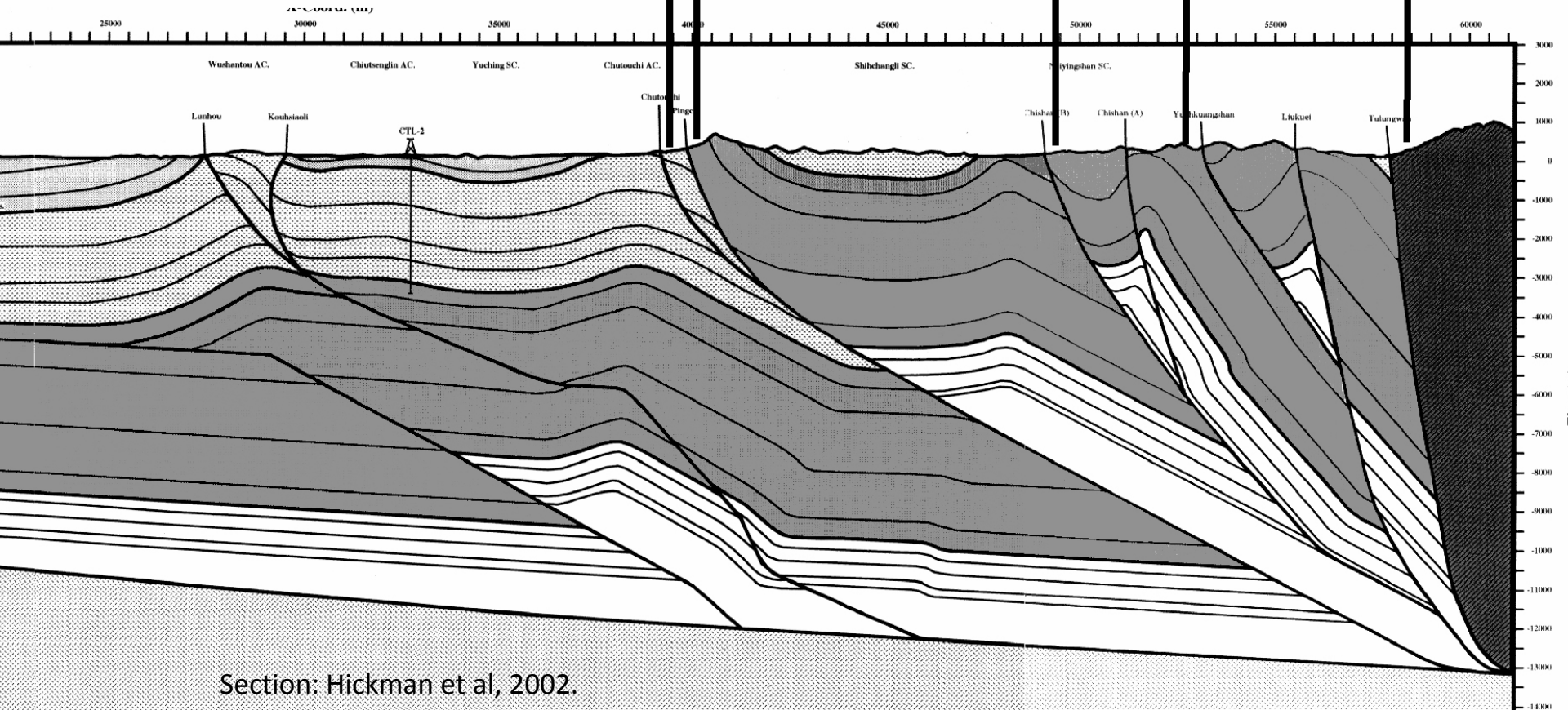

Section: Hickman et al, 2002.

Conclusions

- Oblique collision in Taiwan provides opportunity to measure rates of uplift and erosion.
- Fission track studies indicate erosion rates of 4 to 6 mm/yr.
- Exhumational SS reached for Apatite, but not Zircon.
- Unreset Ar ages implies shallow wedge trajectories.
- Southern Taiwan may exhibit early (2 Ma) cooling.
- Western Taiwan cooling history complicated by thrust-belt structure.